

1. Introduction

The bio-based industry is urged to exploit novel resources with more sustainable value-chains to tackle imminent challenges associated with food security, energy supply, and biodiversity due to a growing world population. Single-cell-based value-chains, including microalgae, with closed resource cycles have gained momentum, owing the sustainability notion of their value-chains. Microalgae find myriad effective or putative applications in food and feedstock production, pharmaceutical, nutraceutical, and biodiesel sectors, and wastewater remediation (Caporgno and Mathys, 2018). However, cultivation costs for microalgae remain high, impairing their economic viability and thus competitiveness on the market (Enzing et al., 2014). Nanosecond pulsed electric field treatment (nsPEF) is a technology-driven, resource-efficient approach to foster single-cell-based value-chains. It could contribute to transform microalgae biorefineries into economically viable concepts. nsPEF treatments bear the benefit of triggering cell proliferation, while being non-thermal and non-invasive. Hence, cell viability and techno-functional properties of cell components are maintained upon processing while simultaneously the energy consumption associated with the process is low (Buchmann et al., 2018). The underlying theory of nsPEF-based growth stimulation assumes that pulses with durations in the ns and amplitudes in the kV-MV range have a more pronounced effect on intracellular structures. They cause abiotic, sublethal stress thereby triggering cell proliferation as shown for *Arthrospira platensis*, axenic phototrophic and heterotrophic *Chlorella vulgaris*, and *Saccharomyces cerevisiae* (Buchmann and Mathys, 2019; Haberkorn et al., 2019; Kotnik and Miklavčič, 2006). Main parameters affecting nsPEF treatment outcomes include the pulse repetition frequency (PRF) f (Hz), the electric field strength E (kV cm⁻¹), the pulse width τ_p (ns), the pulse shape, the pulse number n (-), and the medium conductivity σ (mS cm⁻¹), all affecting the specific energy input W_s (J kg⁻¹) (Buchmann et al., 2019, 2018; Miklavčič, 2017). Growth stimulation of phototrophic *C. vulgaris* in non-axenic cultures, however has not been addressed so far. Cultivation of phototrophic microalgae in monocultures on industrial scale is not realistic, as maintaining axenic cultures under sterile cultivation conditions would neither be economically nor practically feasible (Kazamia et al., 2012). At present, progress in implementing nsPEF for growth stimulation of microalgae in non-axenic cultures and ultimately on industrial scale is hampered by an insufficient understanding of the impact of microalgae-bacteria consortia on the treatment outcomes. Hence, there is lacking knowledge regarding ecosystem responses to treatments or the effect of ecosystem dynamics on the treatment outcome. This can result in unspecific triggering of organisms and thus none-reproducible treatment outcomes (Buchmann and Mathys, 2019; Haberkorn et al., 2020). Therefore, the study aimed at investigating microalgal ecosystem responses to nsPEF treatments. The effect of electric field strength and PRF on the biomass yields was investigated, as main parameters affecting the treatment outcome. In that context, flow cytometry (FCM) has emerged as a leading tool for single-cell ecosystem management, as it allows for a fast and reproducible detection and enumeration of cultivable and non-cultivable taxa. Combining FCM-based monitoring with advanced data analysis, such as phenotypic fingerprinting provides information on community shifts based on phenotypic traits and cellular responses to certain events (Props et al., 2018, 2016).

2. Materials and methods

2.1. Culture maintenance

Chlorella vulgaris SAG 211-12 was obtained as non-axenic culture from the University of Stuttgart (Germany) and maintained as stock culture. Cultivation conditions were adopted from Haberkorn et al. (2019) to allow for comparability of results. Briefly, in 200 mL cultivation volume using modified diluted seawater nitrogen (DSN) medium (141.65 g L⁻¹ NaNO₃), cultures were stored in a shaking incubator (Multitron PRO, Infors AG, Bottmingen, Switzerland) at 25 °C, 150 rpm, 7% v/v CO₂, 70% relative humidity (rH), and a mean photosynthetically

active photon flux density (PPFD) of 36 μmol photons m⁻² s⁻¹ using 500 mL Erlenmeyer flasks (Pohl et al., 1987). Stock cultures were continuously sub-cultured harvesting 100 mL weekly (5 min, 3,000 × g) and inoculated into fresh DSN medium to obtain a 200 mL cultivation volume.

2.2. Experimental cultures

For experiments, 100 mL of culture was harvested (5 min, 3,000 × g) and inoculated to a dry substance (DS) of 0.14 g L⁻¹ (500 mL cultivation volume; 1,000 mL Erlenmeyer flasks) using modified DSN medium. The cultures were maintained in a shaking incubator (25 °C, 150 rpm, 7% v/v CO₂, 70% rH, PPFD = 36 μmol photons m⁻² s⁻¹). For treatments, 50 mL culture batches were segregated into sterile 100 mL Erlenmeyer flasks during the early exponential growth phase (36 h post inoculation). For each treatment condition, duplicate cultures were prepared. Microalgal and prokaryotic growth were monitored manually by FCM-based cell count determination using forward (FSC) and sideward (SSC) scattered light intensities and the nucleic acid content (SYBR® Green I staining), as they were shown to correlate well with actual biomass yields (Haberkorn et al., 2019). Therefore, cultures were diluted with filtered (0.1-μm, Millex-GP, Millipore; Merck KGaA, Darmstadt, Germany) water (Evian; Danone, Paris, France), where necessary, to a total cell concentration below 2.0×10^5 cells mL⁻¹. Samples were stained 1:100 with a SYBR® Green I solution (1:100 in 0.1-μm filtered DMSO; Life Technologies, Eugene, OR, USA), incubated 10 min at 37 °C in the dark, and manually assessed by FCM in duplicates. Nitrate (NO₃⁻) consumption was determined in duplicates following a procedure described elsewhere (Collos et al., 1999; Haberkorn et al., 2019).

2.3. nsPEF treatment

All treatment and process parameters were adapted from Haberkorn et al. (2019). An FPG 10-INL 100 pulse generator with a maximum possible pulse width of 100 ns (FID GmbH, Burbach, Germany) was used for the nsPEF treatments, which were applied three times at 3 h inter-treatment intervals. The specific energy input was determined employing in-depth nsPEF system characterization (Buchmann et al., 2018). The pulse repetition frequency PRF (Table 1A) and the electric field strength E (Table 1B) were assessed during two screening experiments (I, II) to obtain biological duplicates.

2.4. Flow cytometry

All samples were measured on a BD Accuri C6® Plus flow cytometer (BD Accuri Cytometers, San Jose, CA, USA) equipped with a 20-mW laser, emitting at a wavelength of 488 nm. Signals were collected for (1) FSC and (2) SSC light intensities, (3) green fluorescence (FL1; 533 ± 30 nm), and (4) red fluorescence (FL3; 675 ± 25 nm) to reflect (A) cell size, (B) cell granularity, (C) nucleic acid content by SYBR® Green I staining, and (D) chlorophyll autofluorescence, respectively. Fluidics for the flow cytometer were used as indicated by the supplier. Before each experiment, the calibration of the flow cytometer was assessed with calibration beads (BD™ CS&T RUO Beads; BD BioSciences, San Jose, CA, USA). Manual flow cytometer measurements were always conducted with a 50 μL sampling volume, a flow rate of 66 μL min⁻¹, and a lower threshold of 800 on the FL1-H channel.

2.5. Data analysis

Raw data was collected with the BD Accuri C6® software (BD Accuri Cytometers, San Jose, CA, USA). Each sample generated a single FCS file, which was exported into the R statistical environment (R-Studio, v1.1.456). All data and statistical assessment were performed using the functionalities offered by the *flowCore* (v1.38.2) and *PhenoFlow* (v1.1.2) packages following the data processing strategy suggested by Props et al. (2018). Briefly, virtual gating was used to establish microalgal and

Table 1

Process parameters of the Pulse Repetition Frequency PRF (A) and electrical field strength E (B) screening experiments. Electric field strength E (kV cm^{-1}), pulse width τ_p (ns), pulse repetition frequency f (Hz), residence time t (s), and pulse number n (-) are indicated. The specific energy input W_s (J kg^{-1}) is provided for a single treatment. Relative biomass increases (%) of *C. vulgaris* and bacteria 5 days after the treatment are provided as comparison to an untreated control.

	E (kV cm^{-1})	τ_p (ns)	f (Hz)	t^a (s)	n (-)	W_s^a (J kg^{-1})	Relative biomass increase ^a (%)	
							<i>C. vulgaris</i>	Bacteria
A	10	100	3	0.61 ± 0.19	1.83	195.7 ± 61.8	$+42.3 \pm 12.4$	$+69.1 \pm 42.9$
	10	100	5	0.61 ± 0.19	3.04	326.1 ± 102.9	$+35.9 \pm 10.3$	$+96.4 \pm 34.1$
	10	100	7	0.61 ± 0.19	4.26	456.6 ± 144.1	$+50.1 \pm 12.2$	$+77.0 \pm 37.4$
	10	100	9	0.61 ± 0.19	5.48	587.0 ± 185.3	$+47.5 \pm 8.1$	$+23.8 \pm 20.4$
	10	100	7	0.61 ± 0.19	4.26	110.4 ± 34.8	-15.9 ± 13.9	-74.7 ± 15.1
B	5	100	7	0.61 ± 0.19	4.26	441.5 ± 139.3	-17.1 ± 13.8	-82.7 ± 14.6
	10	100	7	0.61 ± 0.19	4.26	993.3 ± 313.5	-29.0 ± 8.1	-82.5 ± 14.7
	15	100	7	0.61 ± 0.19	4.26	1765.8 ± 557.3	-42.2 ± 13.5	-83.8 ± 11.9
	20	100	7	0.61 ± 0.19	4.26			

^a The data are presented as the mean \pm standard deviation ($n = 4$; measured in duplicates).

prokaryotic gates. No compensation was applied. Total cell counts of *C. vulgaris* and bacteria were determined. An unpaired Man-Whitney test was conducted to compare counts obtained from different treatments. For assessing phenotype related shifts within the prokaryotic community, the *fbasis* function was used to first perform bivariate kernel density estimation on the chosen phenotypic traits (FL1-A, FL3-A, FSC-A, SSC-A). Subsequently, density values were concatenated to a one-dimensional vector, the phenotypic fingerprint. Based on the phenotypic fingerprint, beta-diversity was determined (*beta_div_fcm*) using Bray Curtis as distance metrics and ordinated by Principal Coordinate Analysis (PCoA) to compare prokaryotic communities of different treatments based on their phenotypic traits (Props et al., 2016).

3. Results and discussion

A specific energy input of $3 \times 360.15 \pm 114.14 \text{ J kg}^{-1}$ (5 Hz, 100 ns, 10 kV cm^{-1}) was shown to significantly trigger the growth of the same axenic *C. vulgaris* strain 5 days after the treatment, when treating cells during the early exponential growth phase (36 h post inoculation), hence within the fast proliferating state of the cells (Haberkorn et al., 2019). Therefore, screenings applying specific energy inputs between 110.4 ± 34.8 and $1765.8 \pm 557.3 \text{ J kg}^{-1}$ during the early exponential growth phase were conducted in biological and technological duplicates by altering the pulse repetition frequency (Table 1A) and the electric field strength (Table 1B).

3.1. Influence of the pulse repetition frequency

A treatment time point of 36 h post inoculation significantly enhanced *C. vulgaris* biomass yields by $50.1 \pm 12.2\%$ applying 100 ns, 7 Hz, and 10 kV cm^{-1} ($n = 4$; $p < 0.05$) during PRF screening experiments (Table 1A). The obtained biomass yields were higher than those reported for axenic *C. vulgaris* ($17.53 \pm 10.46\%$) (Haberkorn et al., 2019). Prokaryotic presence might thus have positively affected *C. vulgaris* growth performance following nsPEF treatments. The highest prokaryotic growth enhancement however ($n = 4$; $p < 0.005$) was observed at a PRF of 5 Hz ($+96.4 \pm 34.1\%$). Increasing the PRF up to 9 Hz progressively abated the growth enhancing effect of the nsPEF treatments on bacteria (Table 1A). A stronger growth promoting effect on bacteria coincided with initial expectations, as bacteria tend to proliferate faster than microalgae with doubling times usually in the timescale of hours, whereas the doubling time of *C. vulgaris* under the given conditions often ranged between 20 and 25 h in the exponential phase. Assessment of nutrient consumption substantiated those findings. Nitrogen was abated faster in cultures with higher final biomass yields (Fig. 1a–b).

3.2. Influence of the electric field strength

During PRF screening experiments, the highest *C. vulgaris* biomass yield was obtained following nsPEF treatments at 100 ns, 7 Hz, and 10 kV cm^{-1} . Therefore, screenings of different electric field strengths were conducted at

a PRF of 7 Hz and a pulse width of 100 ns. However, during those screenings applying a treatment window of 100 ns, 7 Hz, and 10 kV cm^{-1} resulted in biomass decreases of $-17.1 \pm 13.8\%$ (*C. vulgaris*) and $-82.7 \pm 14.6\%$ (bacteria) 5 days after the treatment. Raising the electric field strength increasingly impaired *C. vulgaris* count development leading to biomass decreases of up to $-42.2 \pm 13.5\%$ at the highest electric field strength of 20 kV cm^{-1} (Table 1B). Bacteria were similarly affected by the different electric field strengths, but counts were significantly and to a higher extent decreased than those of *C. vulgaris* ranging between $-74.7 \pm 15.1\%$ and $-83.8 \pm 11.9\%$ ($n = 4$; $p < 0.05$). In accordance, Buchmann et al. (2018) highlighted the potential of nsPEF for selectively inactivating prokaryotes in *C. vulgaris* cultures. nsPEF treatments of the two screening experiments yielded biomass increases during PRF screenings experiments, while decreases were observed during electric field strength screening experiments albeit applying the same processing conditions (7 Hz, 100 ns, and 10 kV cm^{-1}). Before each screening, initial prokaryotic and microalgal counts were similar and showed a microalgae:bacteria concentration ratio of around 2.5:1. Following nsPEF treatments (5 days post treatment), in the control group of the electric field strength screening experiments concentration ratios shifted in favor of bacteria, leading to a 1:18 microalgae:bacteria concentration ratio. Microalgal and bacterial cell counts were elevated 2-fold and 71-fold, respectively in the control group of electric field strength screening experiments if compared to PRF screening experiments. In the treated samples (7 Hz, 100 ns, and 10 kV cm^{-1}) however, the microalgae:bacteria concentration ratio only amounted to 1:4, indicating that the nsPEF treatments allowed to selectively abate prokaryotic counts. During the screenings of the PRF, microalgae remained dominant resulting in a 2:1 microalgae:bacteria ratio, both within the control, as well as the group treated at 7 Hz, 100 ns, and 10 kV cm^{-1} . As initial microalgae:bacteria ratios and concentrations (microalgal and prokaryotic counts: $1.1 \times 10^4 \pm 1.5 \times 10^3$ and $4.3 \times 10^3 \pm 9.1 \times 10^1$ or $1.2 \times 10^4 \pm 1.4 \times 10^3$ and $4.9 \times 10^3 \pm 8.2 \times 10^2$ cells μL^{-1} during the screening of the PRF or the electric field strength, respectively) were similar for all screening experiments, it was hypothesized that a shift in prokaryotic community diversity affected prokaryotic and microalgal growth dynamics and ultimately the nsPEF treatment outcome.

3.3. Prokaryotic community changes assessed by phenotypic fingerprinting

To investigate the relation of prokaryotic community diversity and nsPEF treatment outcome, phenotypic fingerprinting was employed as a novel approach for assessing population dynamics in microalgal ecosystems. The determination of phenotypic fingerprints of a microbial community reflects its diversity based on phenotypic or metabolic traits. Accordingly, the diversity depends, amongst other factors, on cell morphology or cellular metabolic states. A PCoA based assessment of bacterial beta-diversity of phenotypic fingerprints indicated that prokaryotic community diversity was similar before the treatments, i.e., in the backup culture for screening trials of the PRF and the electric field

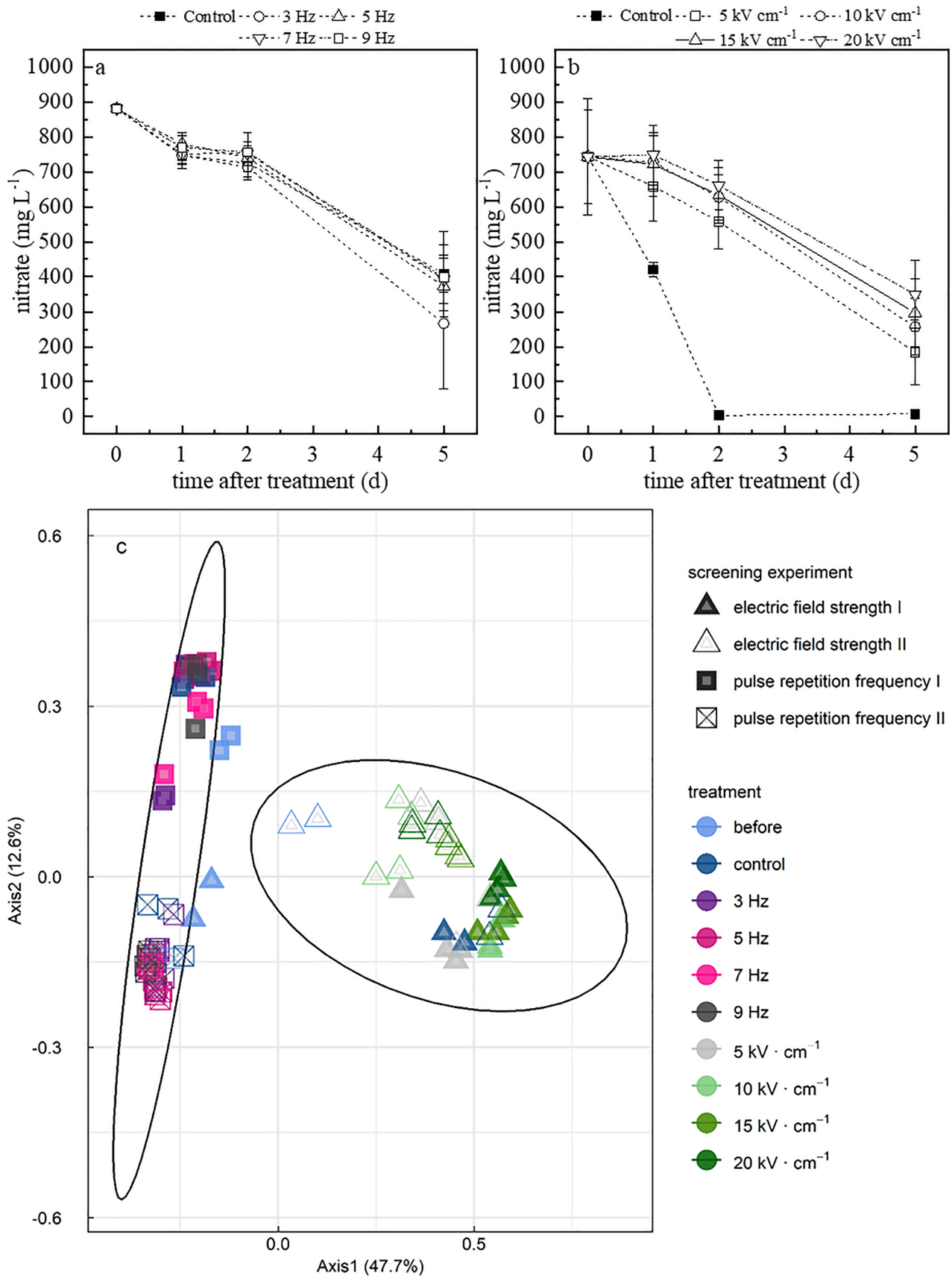


Fig. 1. Nitrate consumption and PCoA of prokaryotic phenotypic fingerprints following nsPEF treatments. Nitrate consumption during screening experiments of the pulse repetition frequency (a) and the electric field strength (b). The data are presented as the mean ± standard deviation (n = 4; measured in duplicates). PCoA (c) of prokaryotic phenotypic fingerprints before and 5 days following nsPEF treatments. Each point represents an individual sample obtained after the two screening experiments (I, II) for the pulse repetition frequency (⊠) and the electric field strength (Δ) (n = 4 for each treatment condition; measured in duplicates).

strength (100 ns, 7 Hz, and 10 kV cm⁻¹), but differed 5 days following treatments (Fig. 1c). Since results for PRF and electric field strength screening trials were reproducible in biological replicates, diversity related community changes that affected the treatment outcome might have occurred between the two screening trials. Changes in prokaryotic community diversity relate to shifts in either ecosystem richness or evenness. Haberkorn et al. (2020) showed that community diversity remains largely unaffected over elongated cultivation periods and under varying cultivation conditions, indicating that changes in community evenness might not have triggered the observed differences in the treatment outcome. Shifts in ecosystem richness, i.e., a change in the number of different phenotypic or metabolic traits might relate to the number of different species present in the prokaryotic community. An extraneous invasion of bacterial species during stock-culture maintenance and between screening trials of the PRF and the electric field strength could have affected ecosystem richness and consequently phenotypic fingerprints. The data indicates that on day 5 of cultivation, prokaryotic communities employed for the screening of the electric field strength differed in their phenotypic diversity if compared to the prokaryotic community of the PRF screening. Hence, although not distinguishable through phenotypic fingerprinting owing a similarity in phenotypic and metabolic traits in an early growth stage, changes emerged at a later growth stage. Hence, advanced data analysis of FCM data derived from prokaryotic communities substantiated the initial hypothesis that changes in prokaryotic community diversity affected the nsPEF treatment outcome. The obtained data show that nsPEF treatments have the potential for increasing biomass yields of *C. vulgaris* also in non-axenic cultures and also that of prokaryotic counts. However, the data also showed that bacterial community composition is crucial for reproducible nsPEF treatment outcomes and can govern either growth promotion or selective inactivation. The difference in bacterial community diversity resulted in improved growth of especially bacteria in the control group during the screening of the electric field strength, while rendering prokaryotic populations more susceptible to an inactivation by nsPEF. Although the assessment of phenotypic fingerprints provided valuable insights for investigating the relation of prokaryotic community diversity and nsPEF treatment outcome, it only provides a first step in understanding potential underlying treatment mechanisms. Next generation based 16S rRNA sequencing could provide a tool to substantiate the obtained findings on a taxonomic base. Engineered microalgal-bacteria ecosystems coupled with metabolic studies could then aid in advancing the application of nsPEF in non-axenic microalgae cultures through providing controlled and in-depth insights into underlying treatment mechanisms. Ecological engineering approaches could build on those findings to tailor bacterial communities that foster microalgal growth, while also being selectively inactivable. The obtained findings can pave the way for advancing the industrial realization of nsPEF, as they provide a base for an improved understanding of microalgal-bacterial ecosystem dynamics following nsPEF treatments and thus aid in leveraging process control. Thereby, the study highlights the importance of combining nsPEF treatments with high throughput on- and inline monitoring and ecosystem management tools, such as FCM. However, these observations remain subject to further in-depth investigations. Incorporating biotechnology governed approaches, envisioning a bacterial community tailored towards growth stimulation and/or selective inactivation into nsPEF-based biorefinery concepts could aid in leveraging microalgae up-, or downstream processing and thus advance microalgal feedstock production. Understanding ecosystem dynamics following nsPEF treatments has implications not only for microalgal biorefineries, but also for myriad applications relying on single-cell value-chains in the bio-based domain.

4. Conclusions

NsPEF treatments can leverage microalgal biomass also in non-

axenic cultures. A processing window of 100 ns, 7 Hz, and 10 kV cm⁻¹ increased phototrophic *C. vulgaris* (+50.1 ± 12.2%) and bacterial yields (+77.0 ± 37.4%). Altering bacterial diversity decreased *C. vulgaris* (-17.1 ± 13.8%) and bacterial counts (-82.7 ± 14.6%) applying the same processing window. PCoA of phenotypic fingerprints indicated that bacterial diversity governed that outcome. The study highlights the potential impact of combining ecological engineering with nsPEF processing for growth stimulation/selective inactivation to foster the upsurge of industrial nsPEF realization and ultimately the economic viability of single-cell-based biorefineries.

Declaration of Competing Interest

The authors declare that they have no known competing financial interests or personal relationships that could have appeared to influence the work reported in this paper.

Acknowledgement

The authors gratefully acknowledge Prof. Dr. Erich Windhab from the ETH Zurich Food Process Engineering Laboratory and the ETH Zürich Foundation for their support.

Appendix A. Supplementary data

Supplementary data to this article can be found online at <https://doi.org/10.1016/j.biortech.2020.124173>.

References

- Buchmann, L., Böcker, L., Frey, W., Haberkorn, I., Nyffeler, M., Mathys, A., 2018. Energy input assessment for nanosecond pulsed electric field processing and its application in a case study with *Chlorella vulgaris*. *Innovative Food Sci. Emerg. Technol.* 47, 445–453. <https://doi.org/10.1016/j.ifset.2018.04.013>.
- Buchmann, L., Frey, W., Gusbeth, C., Ravaynia, P.S., Mathys, A., 2019. Effect of nanosecond pulsed electric field treatment on cell proliferation of microalgae. *Bioresour. Technol.* 271, 402–408. <https://doi.org/10.1016/j.biortech.2018.09.124>.
- Buchmann, L., Mathys, A., 2019. Perspective on Pulsed Electric Field Treatment in the Bio-based Industry. *Front. Bioeng. Biotechnol.* 7, 1–7. <https://doi.org/10.3389/fbioe.2019.00265>.
- Caporgno, M.P., Mathys, A., 2018. Trends in microalgae incorporation into innovative food products with potential health benefits. *Front. Nutr.* 5, 1–10. <https://doi.org/10.3389/fnut.2018.00058>.
- Collos, Y., Mornet, F., Sciandra, A., Waser, N., Larson, A., Harrison, P.J., 1999. An optical method for the rapid measurement of nitrate in marine phytoplankton cultures. *J. Appl. Phycol.* 11, 179–184.
- Enzing, C., Ploeg, M., Barbosa, M., Sijtsma, L., 2014. Microalgae-based products for the food and feed sector: an outlook for Europe. JRC Scientific and Policy Reports, no. In: JRC, 85709. Joint Research Centre, Luxembourg, p. 82 – pp.
- Haberkorn, I., Böcker, L., Mathys, A., Walser, J., Helisch, H., Belz, S., Fasoulas, S., Schuppler, M., 2020. Characterization of *Chlorella vulgaris* (Trebouxiophyceae) associated microbial communities. *J. Phycol.* 1–14. <https://doi.org/10.1111/jpy.13026>.
- Haberkorn, I., Buchmann, L., Hiestand, M., Mathys, A., 2019. Continuous nanosecond pulsed electric field treatments foster the upstream performance of *Chlorella vulgaris*-based biorefinery concepts. *Bioresour. Technol.* 293, 122029. <https://doi.org/10.1016/j.biortech.2019.122029>.
- Kazamia, E., Czesnick, H., Nguyen, T.T.V., Croft, M.T., Sherwood, E., Sasso, S., Hodson, S.J., Warren, M.J., Smith, A.G., 2012. Mutualistic interactions between vitamin B12-dependent algae and heterotrophic bacteria exhibit regulation. *Environ. Microbiol.* 14, 1466–1476. <https://doi.org/10.1111/j.1462-2920.2012.02733.x>.
- Kotnik, T., Miklavčić, D., 2006. Theoretical evaluation of voltage inducement on internal membranes of biological cells exposed to electric fields. *Biophys. J.* 90 (2), 480–491. <https://doi.org/10.1529/biophysj.105.070771>.
- Miklavčić, D., 2017. Handbook of Electroporation. *Handb. Electroporation* 1–4, 1–2998.
- Pohl, P., Kohlhase, M., Krautwurst, S., Baasch, K.-H., 1987. An inexpensive inorganic medium for the mass cultivation of freshwater microalgae. *Phytochemistry* 26 (6), 1657–1659.
- Props, R., Monsieus, P., Mysara, M., Clement, L., Boon, N., Hodgson, D., 2016. Measuring the biodiversity of microbial communities by flow cytometry. *Methods Ecol. Evol.* 7 (11), 1376–1385. <https://doi.org/10.1111/2041-210X.12607>.
- Props, R., Rubbens, P., Besmer, M., Buysschaert, B., Sigris, J., Weilenmann, H., Waegeman, W., Boon, N., Hammes, F., 2018. Detection of microbial disturbances in a drinking water microbial community through continuous acquisition and advanced analysis of flow cytometry data. *Water Res.* 145, 73–82. <https://doi.org/10.1016/j.watres.2018.08.013>.